ARTICLE TEMPLATE

Electromagnetic tracking of endoscopic ultrasound probe for pancreas examination: accuracy assessment under realistic medical conditions

Jean-Paul Mazellier[a, b] and Cindy Rolland[a] and Emilie Wernert[a] and Julieta Montanelli[a] and Lee Swanstrom[a] and Benoit Gallix[a] and Leonardo Sosa Valencia[a] and Nicolas Padoy[a, b]

[a]IHU Strasbourg, France; [b]ICube, University of Strasbourg, CNRS, France

ARTICLE HISTORY
Compiled September 14, 2022

ABSTRACT
Pancreatic cancer, due to poor survival rates, stands as the 3^{rd} cause of death by cancer in 2021 and is predicted to become 2^{nd} in 10 years from now. In this context, early tumors diagnosis is primordial but unfortunately standard 3D medical imaging methods fail to reach the required sensitivity. Endoscopic ultrasound (EUS) stands as an alternative. This technique, however, is not widely available due to its difficulty to master, in particular with respect to the mental spatial positioning of the EUS probe. We focus on developing a tool that could provide low EUS expertise endoscopists with a guidance system that would make spatial navigation of the probe much easier. This would be enabled by providing a computer assisted rendered scene showing patient's 3D model, registered on the patient current examination position. The scene would also integrate a real-time representation of the EUS probe registered in real-time. The corresponding accuracy is largely relying on the efficient registration of the patient specific model (pre-examination CT scan in this study) to the real patient pose during EUS examination. For that purpose, we developed and tested an electromagnetic tracking system attached to an EUS probe that can be operated for pancreas screening. We detail the used registration algorithm and our original experimental method for EUS probe pose accuracy measurement based on Cone Beam Computed Tomography (CBCT). These methods have been deployed on different models such as phantom and swine. We demonstrate an accuracy in position and angle of respectively 10.4 ± 4.0 mm and $8.7° \pm 4.1°$ in pre-clinical conditions. We also demonstrate that efficient navigation can be proposed to the clinician during EUS even in complex and realistic anatomy of a swine model. This work is paving the way to a guided EUS navigation system for pancreatic cancer examination.

KEYWORDS
Pancreas ; Ultrasound ; Endoscopic Ultrasound ; Navigation ; Electromagnetic tracking ; Augmented Reality

1. Introduction

Worldwide, the number of pancreatic cancer detection is doubling every decade since the 90's, mostly in 50^{+} years old population, irrespective of gender (Huang et al. 2021). While being of relatively low prevalence in population, being ranked 7^{th} worldwide, this

CONTACT J.-P. Mazellier. Author. Email: jean-paul.mazellier@ihu-strasbourg.eu

cancer type is associated with a dramatically high mortality rates. This makes pancreas cancer the 3^{rd} cause of death by cancer nowadays, and it is predicted to become the second cause in one decade from now. Such dramatic figures are linked to the correlation of 5-year survival rate with tumor size at diagnosis time, namely less than 5% versus up to 80% for respective tumor sizes of 20mm and 10mm (Ferlay et al. 2019). This points out that early diagnosis is a key factor in patient prognosis. Unfortunately, standard 3D medical imaging such as CT scanner and MRI fail to efficiently detect pancreatic tumors less than 20mm. Currently, only endoscopic ultrasound (EUS) is able to provide a reliable diagnosis for tumors down to 5mm(Huang et al. 2021). Moreover, EUS is able to biopsy small lesions with more than 85% accuracy allowing a clear diagnosis before pancreatic surgery which is the only curative treatment today available (Huang et al. 2021). However, such efficiency in diagnosis is up to date limited to EUS experts practitioners. But expertise in the field of EUS comes at the price of a large number of total performed cases by practitioner (estimated to few thousands of examination) which significantly limits general access to worldwide population. This high number of cases is related both to complex ultrasound image interpretation during examination but also to complex manipulation of the flexible endoscope to ensure controlled motion for the EUS probe for complete scanning of the pancreas. Indeed, as the probe navigation by the EUS practitioner is mostly based on US image (pancreas is probed through stomach/duodenum wall with no direct optical access), long practice is mandatory to ensure this mastery. In this context, a computer assisted guidance tool for EUS probe navigation would help spreading efficient and consistent EUS pancreas examination.

2. Related work

Different works have focused on providing physicians with tool guidance. For instance, optical tracking has proven to be efficient in rigid instruments navigation (Allan et al. 2014; Xiao et al. 2018). But in our case, and because of the flexible nature of the EUS endoscope, the complete deformation of the scope would require strong assumptions associated with complex interaction to oesophagus tube and stomach wall during examination. In order to encompass such difficulty, simultaneous localization and mapping (SLAM) based navigation is a common way to provide in-body navigation (Münzer et al. 2018). But in case of EUS this approach would be very challenging away from the oesophagus because the stomach wall (where most of the time EUS probe stays in, along with duodenum) is highly deformable and also because significant time of EUS examination is performed with the probe in contact to tissue (for US propagation through tissues), meaning no spatial information can be retrieved from the endoscopic camera. Other navigation methods have been developed which rely on non-line of sight tracking techniques. For instance, optical fiber based shape tracking has recently benefited from renewed interest in medical application (Jäckle et al. 2019; van Herwaarden et al. 2021; Floris et al. 2021) as it offers advantages in terms of compactness and robustness to environmental perturbation. Nevertheless, this technology is still expensive and would not fit with the affordable approach we target. Electromagnetic (EM) tracking also offers the possibility to track the sensor without direct visual access and has proven to be efficient in diverse clinical applications (Franz et al. 2014). We can also cite the Olympus ScopeGuide system Olympus (2022) allowing for real-time colonoscope shape tracking, helping clinician to detect endoscope loop and avoid any tissue damage. However this representation is not regis-

tered to a patient model and thus is not dedicated to direct probe navigation. In order to navigate an instrument into patient body, a registration approach must be used. Some works have focused on using EM tracking to specifically navigate flexible EUS probe. In (Hummel et al. 2008), authors use a combination of EM tracker information with US image registration to prior CT/MRI volume with proven accuracy down to 5mm. However, development are restricted to a test bench with no demonstration in a realistic model. Work of (Bonmati et al. 2017) focused on the influence of the active EUS probe on the EM sensor accuracy and demonstrated sub-millimetric induced error by the activation of the piezoelectric elements in the EUS probe; still, this work was not performed in realistic medical environment with other representative disturbance sources. In Estépar et al. (2007), authors consider a EUS surgical application with accuracy target of 5mm by using EM tracking of EUS probe. They studied, in porcine model, multiple effects such as respiration and develop an in-body accuracy method using venous tree US imaging compared to a prior CT scan counterpart. They also use an extra EM sensor to keep track of patient body in order to update the EM to CT frame rigid registration through procedure. This work paved the way to navigated EUS procedure. Moreover, it suffers multiple impractical limitations for clinical use due to the calibration procedure, the EM tracker to EUS probe registration, lasting about one hour and with complex registration in between CT and EM frames.

In the present study, we want to evaluate an approach that provide clinicians with a "GPS-like" guidance tool where the probe is navigated efficiently in the proximity of the pancreas gland, whose pose is rendered in virtual reality, with EUS probe pose accuracy coherent with the aforementioned task. Our development have been done in order to prepare a clinical trial to test our system on patients. So clinical constraints (material disinfection, tracked EUS probe preparation time, etc.) have been taken into account at the earliest stage. Based on EM tracking, we developed building bricks to develop an augmented reality tool for providing endoscopists, with no or little EUS practice, with a guidance tool to perform efficient EUS examination. Our goal here is to help this category of practitioner to navigate faster and with more confidence to the pancreas as well as getting better spatial representation of the probe with respect to the pancreas for ensuring better coverage of the pancreatic gland during search for potential small lesions.

3. Navigation principle

3.1. Requirements definition

Before any experiment, we defined with clinical experts the minimal accuracy requirements for a guided EUS pancreas examination system. Based on geometrical consideration and assuming typical distance of the probe to the pancreas of 2cm during US examination (stomach wall separation thickness), as well as assuming a typical 10cm length of the gland, we obtained the upper limits for the EUS probe positioning system to be a spatial error less or equal to 25mm and a maximum angle error less or equal to 20°. A system offering accuracy within these bounds would ensure the pancreas to be in the US region of interest under realistic examination conditions. Also, as we target clinical trial, realistic medical constraints have been taken into account. In particular we defined some of our system must-have features which includes: (1) compliance of our system to disinfection procedures; and (2) simple and quick mounting at patient bed.

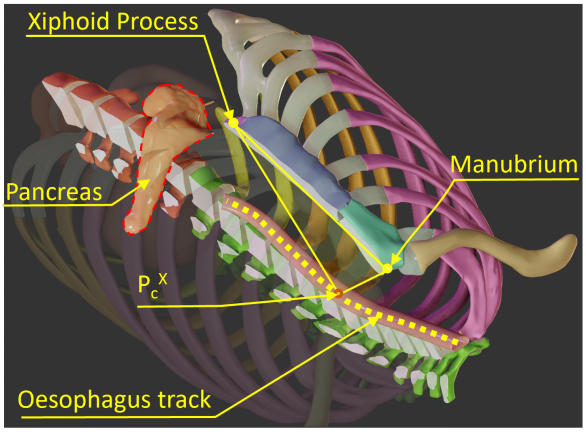

Figure 1. Illustration the inputs of our registration algorithm. In each frame (CT scan and EM), we acquire the Xiphoid Process and Manubrium points (yellow markers) as well as the Oesophagus track (dashed yellow line). For each frame X (in [CT;EM]) we obtain P_c^X (orange marker) which is the closest point in oesophagus track to Manubrium.

3.2. Registration algorithm

Once these specifications were defined, we considered the clinical scenario that would encompass our system use. Before being prescribed a pancreas EUS examination in our medical institute, patients systematically undergo a thoracic-abdominal CT scanner in decubitus supine position (patient lying on his/her back). Contrary to this, EUS examination is generally performed on lateral decubitus position. Nevertheless, patient are moderately sedated during EUS exam for their convenience and for allowing medical staff to perform intubation if ever required. This allows to consider performing the examination in decubitus supine position, and so getting patient pose very close to the one used for CT scan acquisition. This particular EUS examination configuration makes simpler the registration from the patient's CT scan to the patient's body during examination, without involving complex CT scan deformation to fit to very different poses. Multiple options would then be available to perform such registration, but here we take advantage that, in order to reach stomach cavity and duodenum, the EUS practitioners need to insert first the EUS flexible all along oesophagus track. During this step, we can advantageously acquire the EUS probe trajectory, which gives us access to a materialization of the oesophagus track in EM frame (which is attached to EM field generator, see Figure 3). Our purpose is then to register patient CT scan in EM frame based on this EM oesophagus track. Here, we got inspired by previous work of Vemuri *et al.* (Vemuri et al. 2016), who developed a method to register two distinct endoscope head trajectories, obtained with EM tracking, in patient oesophagus from different procedures separated through time. In our study, registration between oesophagus tracks is performed from (1) EM points, and (2) CT scan oesophagus track. Note that (1) is obtained with EM tracking during EUS probe insertion from throat to stomach, while (2) is obtained by selecting 3 points, homogeneously spread on about 20cm of oesophagus track in patient CT scan. Based on these 3 points, a 2-segments path is defined to materialize patient oesophagus in CT scan. In addition to endoscope head EM tracker, authors added two EM trackers on the sternum, respectively at Jugular Notch and nearby Xiphoid Process. Here, these sensors' information has been replaced with single position pointing of Manubrium and Xiphoid Process in EM frame (with use of an EM tracked needle) and corresponding points in patient CT scan

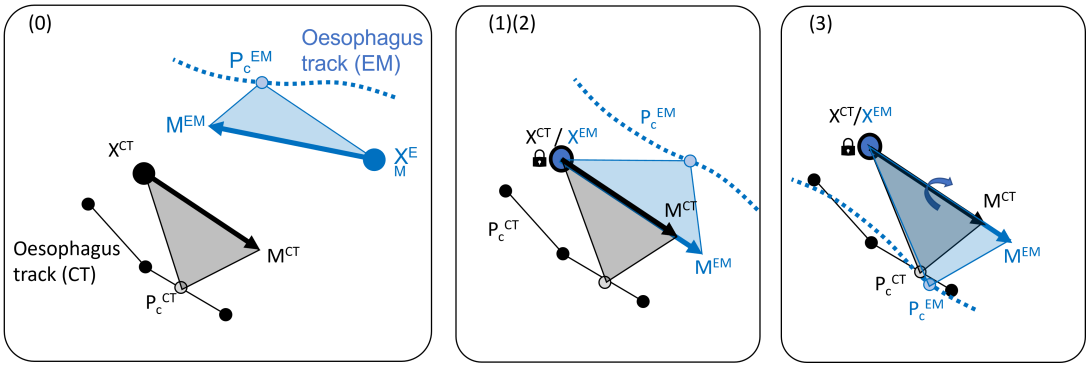

Figure 2. Illustration of our registration algorithm. Step (0) is data acquisition in both frames (CT and EM). Step (1) is Xiphoid Process superimposition and anchoring. Step (2) is Xiphoid Process-Manubrium vectors alignment. Step (3) is triangle Xiphoid Process - Manubrium - P_c^X planes alignment.

(cf Figure 1). Again adapting from (Vemuri et al. 2016), for each frame (resp. EM and CT) we identify in oesophagus track the closest point to Manubrium, denoted as P_c (resp. P_c^{EM} and P_c^{CT}). Note that if Vemuri *et al.* (Vemuri et al. 2016) have chosen to anchor points clouds with respect to the Manubrium, our choice of Xiphoid Process as anchoring point is motivated by the fact that it stands closer to the pancreas, which therefore reduces registration error by lowering the lever effect for pancreas nearby region. Our registration algorithm inputs are illustrated in Figure 1.

Registration between point datasets is then obtained from the following steps, as illustrated in Figure 2:

(1) matching and anchoring Xiphoid Process in both frames (fixing 3 degree of freedom)
(2) aligning Xiphoid Process to Manubrium vectors (fixing 2 degree of freedom)
(3) rotating points clouds to match planes defined by {Xiphoid Process - Manubrium - P_c} while minimizing P_c^{EM} to P_c^{CT} distance (fixing 1 degree of freedom).

3.3. Calibration

To offer EUS probe positioning, the rigid transformation matrix in between the EM tracker and the EUS probe is to be obtained. For that purpose, we use a mechanical calibration jig to obtain such matrix prior to any navigation. The EM tracking system is an NDI-3D Guidance trakStar2. The navigation EM tracker (NDI-3D Guidance PM180) is attached to EUS probe (Pentax EG38J10UT with linear US probe) with two rubbers to firmly maintain the sensor during the examination. The tracked EUS probe is then fitted in a 3D printed calibration jig (which possesses an EUS probe counter-fingerprint) where it is maintained mechanically. The jig is also equipped with three EM reference sensors (NDI-3D Guidance PM800) which allow to retrieve the jig pose in the EM frame. The EUS probe position in jig being known by design, the calibration matrix, associated with the position of the EM tracker fixed on the EUS probe, can be computed. Illustration of the calibration setup is provided in Figure 3. Note that the whole calibration procedure takes about 5 minutes in total.

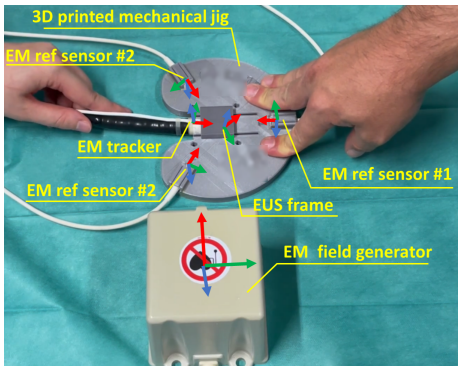

Figure 3. Illustration of 3D printed calibration jig (grey parts in picture) and associated calibration procedure. The calibration procedure is meant to provide the rigid transformation between EM tracker frame and EUS frame. Note that on the picture, the EUS probe is under the 3D printed fixing cover.

4. Experiments and results

In this section, we detail our experiments and provide measurement results as well as 3D scene renderings, both being based on the Slicer 3D software (Kikinis et al. 2014).

4.1. Registration assessment in phantom

We started our navigation trials by using a home-made gelatin phantom, based on a torso gelatin phantom from Clear Ballistics (cf Figure 4). This phantom is added with an oesophagus modeled as a straight tubular cavity, 2cm in diameter and 20cm long. This oesophagus model leads to a cavity moulded on a swine's stomach. A microbubble modified gelatin structure mimicking pancreatic parenchyma in US modality has been inserted few centimeters (1-2cm) away from the inferior stomach cavity wall. In this pancreas-like gelatin portion, two glass marbles (1 centimeter diameter) have been inserted for simulating target lesions. On phantom surface, two physical markers, representing Xiphoid Process and Manubrium, as well as four radio-opaque control markers, for later accuracy control, have been placed. Following the registration procedure described in section "Navigation principle", we acquired oesophagus track and Xiphoid Process / Manubrium data points in EM frame. Defining phantom CT counterpart datapoints, we ran our registration algorithm and obtained an EM to CT rigid transformation matrix. In order to assess the registration accuracy with this approach, different external control marker poses in between both modalities have been compared. EM pose have been obtained using a Civco eTrax EM tracked needle, while CT pose have been obtained from coordinate retrieval in 3D volume. Note that these points have not been used for registration matrix calculation and thus offer independent measurements of registration accuracy. We report in Figure 4 the pose error between control CT markers and registered EM data points from these external markers for 9 experiments obtained from full permutation of 3 different sets of CT scan selected points with 3 different sets of EM recorded point clouds.

It can be observed that, whatever the control point considered, the error remains below a value of 25mm, which is our specification in position accuracy. In addition to this external marker based registration assessment method, we proceeded to navigation of the EUS probe based on real-time rendering of the EUS probe model into the CT scan 3D volume. The goal here was to qualitatively assess that a target (glass

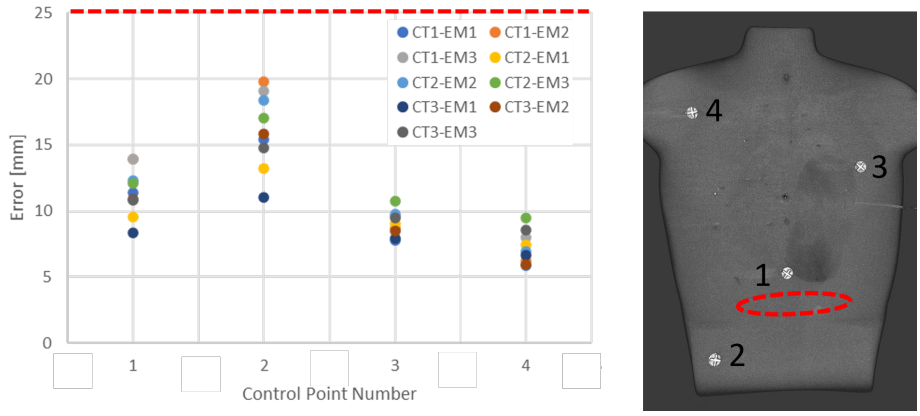

Figure 4. Registration accuracy assessment during phantom experiment based on external control markers matching. Projected pancreas position is indicated (dashed red ellipsoid) for reader's convenience.

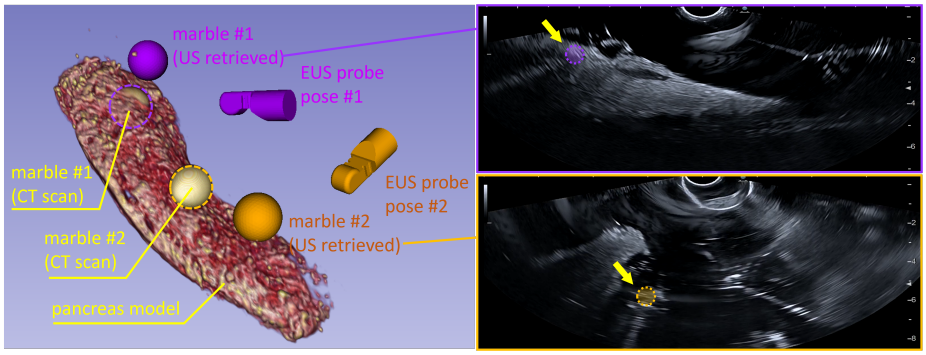

Figure 5. Guided navigation on gelatin phantom for qualitatively retrieving pre-defined targets (glass marbles). Left : 3D rendering of EUS probe, pancreas-like gelatin and target marbles. Rendering is provided for poses of the EUS probe, one for each target. Right : synchronized US image. Estimated marble position is provided (dashed circle) for reader's convenience.

marble) could be efficiently reached based on the provided guidance. We report on Figure 5 3D pose renderings of EUS probe, registered to the CT scan volume, with respect to pancreas model, with its associated tumor-like glass marbles, in parallel to synchronized US images. The two available glass marble targets have been considered here. One can clearly see the characteristic echoing signal of the marble glass in the US view. Note however that the glass marble are not visible by themselves in US image. Based on US observation, approximate glass marble positions can be projected as depicted in Figure 5. We have recomputed the experiment twice for each glass marble and measured the error between the estimated target retrieved positions and corresponding CT scanner positions. This resulted in a re-projection error of 26.2 $\pm$ 2.2 mm. Note that a non-negligible part of this error can be attributed to position estimation of the marbles in the US view because only their echoing is identified, not the glass marble by themselves. Based on this encouraging results, we proceeded with swine model experiments.

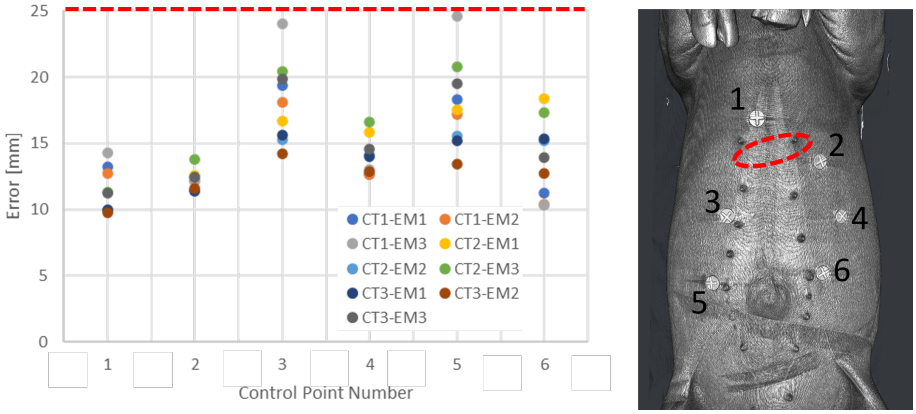

Figure 6. Registration accuracy assessment during swine experiment based on external markers matching. Projected pancreas position is indicated (dashed red ellipsoid) for reader's convenience.

4.2. Registration assessment in swine model

We reproduced previous experiment in a swine model with prior injection of metallic fiducials (ECHO-22-F Cook Medical of typical dimension 5 mm x 0.43 mm), being both radio-opaque and echo-opaque, in pancreas and proximal lymph nodes. These fiducials stood as targets for navigation control purposes. As done on phantom experiment, distance error between EM and CT coordinates of external control markers (previously positioned on swine skin) has been calculated. We present our measurements on Figure 6.

Here, a spatial error of less than 25mm has also been obtained. These first experimental proof of registration accuracy are encouraging, so we wanted to assess for probe pose accuracy on more realistic condition, *i.e.* inside swine stomach, to mimic our foreseen clinical conditions.

In order to provide with medically relevant accuracy values, we proceeded with the following experiment. First, a CT scan of swine model in decubitus supine position is acquired (simulating pre-EUS examination control CT scan of patient). Prior to the CT scan, multiple external control markers have been placed for later registration references. Then we moved the model in an other room equipped with a robotized C-arm. EUS probe calibration and registration have been performed (EUS probe registered in swine CT scan). While keeping the EUS probe inserted in swine stomach, we acquired a Cone Beam Computed Tomography (CBCT) volume, while making sure the EUS probe was in the CBCT volume as well as at least 3 external skin markers for CBCT to CT registration purposes. By proceeding with the rigid transformation of CBCT to CT scan, we obtained CBCT based pose estimation of the EUS probe (internal structure) in the swine model. Based on the EUS piezoelectric array position and orientation, EUS head envelope pose in registered CBCT has been derived. From this registered envelope to our EM base EUS head pose estimation, we derived mismatch parameters defined as distance shift and angle mismatch. Distance shift is the euclidean distance in between US focal spot defined by the center of the semi-circular piezoelectric curvilinear module. Angle shift is defined as the angle between normal vector of both semi-circular base plane (corresponding to US plane). From 6 different poses of the EUS probe in swine stomach, an average distance shift and angle mismatch of respectively 10.4 ± 4.0 mm and $8.7° \pm 4.1°$ have been obtained. On Figure 7, we reported a representation of typical elements such as CBCT-based

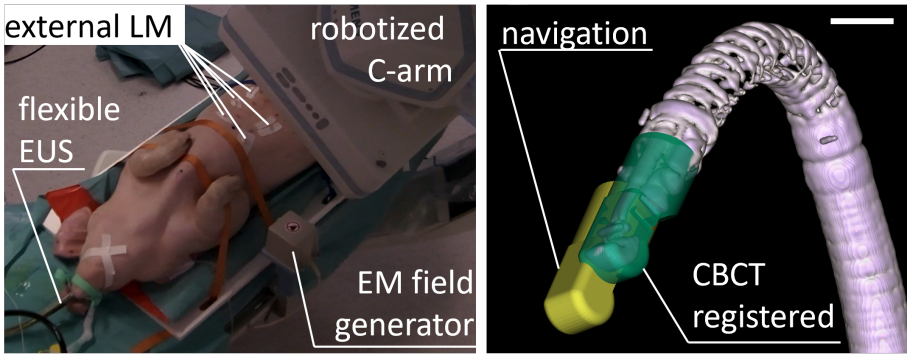

Figure 7. Left: Experimental setup used for navigation and registration accuracy assessment. Right: example of a navigation result compared to a CBCT based representation of the EUS probe. Scalebar is 1cm.

EUS head volume (internal structure) with associated registered EUS head envelope (semi-transparent green surface) as well as our EM-based EUS head pose estimation (opaque yellow surface).

4.3. Evaluation of guidance accuracy during EUS examination

After registration assessment, we focused on the added value of our solution in terms of EUS navigation. To this purpose, we proceeded with the following experiment: fiducials (both radio-opaque and ultrasound-opaque) have been introduced in swine pancreas prior to CT scan. They can be clearly identified in the corresponding acquired volume. During navigation, the EUS practitioner reached some of these fiducials by finding them using US imaging. We then compare the position of the fiducial in CT rigid model to the position as calculated from EUS probe pose. We represent results of such fiducial retrievals in Figure 8. We observed three fiducials (one in pancreas head and two in pancreas body) and respective distance in CT frame have been estimated to 47.4mm, 33.9 mm and 26.6 mm respectively (cf Figure 8), leading to an accuracy estimate of 35.9 ± 10.5 mm. Note that these values are higher than the ones measured from previous CBCT-based registration experiment. We however noticed that fiducial position was always coherent with EUS probe orientation, meaning that we did always observe the registered US-retrieved fiducial in front of sensing US part of EUS probe. We interpret this by noticing that, during EUS examination, some pressure is applied by EUS probe to the tissues in order to ensure good contact for US propagation. This pressure can be one reason for apparent movement of the fiducial with respect to CT-based pose, and the displacement of the fiducial ahead of EUS probe sensing zone is coherent.

5. Discussion and conclusion

Here it has first to be emphasized that, due to our EM tracking system, particular care has been paid to limit environmental perturbations. Indeed these are known to limit EM sensor accuracy with regard to manufacturer specification. These specifications are obtain in perfectly controlled situation with no interfering metal parts nearby EM sensor, which is not the case in medical examination room or in our case due to the vicinity of sensor to EUS probe. We used our system in radio-compatible conditions by

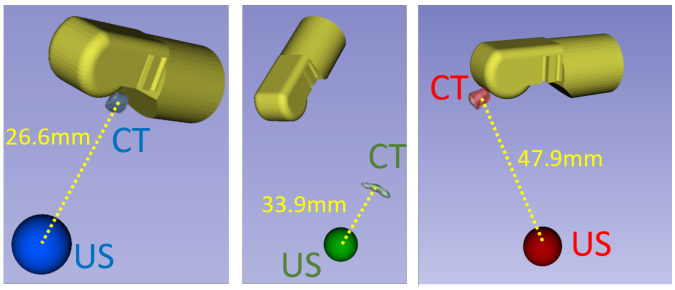

Figure 8. Different EUS probe pose rendering when fiducials was visible in US image. The rendering displays the EUS probe pose and associated fiducial re-positioned from US image as well as CT-based pose of the corresponding ficudial. Left: fiducial in pancreas head; Middle and Right: fiducials in pancreas body.

performing navigation on interventional radiology surgery tables, used as examination table, because their core is made of carbon fiber and not bare metal. Carbon fiber is much less prone to induce EM perturbation compared to metal parts and thus are more suited to our application. Note that this constraint is however compatible with a realistic clinical workflow where a significant number of patients may undergo ERCP (endoscopic retrograde cholangiopancreatography) which involves X-ray imaging and thus requires the use of a radiocompatible examination bed. Such bed are then available in EUS examination centers. We also pointed out that the EM tracker is attached on top of the EUS probe. We could have placed EM tracker in EUS flexible user channel, but this option presented the disadvantage of introducing a much larger error in EM tracking and furthermore, such configuration would have impeded any biopsy during the EUS examination which in turn would have significantly reduced the interest in providing a guidance tool for EUS procedures.

Our registration algorithm has been developed to fit a pre-examination CT scan of the patient, here modeled by phantom and swine models, to EM frame based on the use of the oesophagus track and two external anatomical landmarks present on the patient sternum (Xiphoid Process and Manubrium). We assumed the transformation to be rigid and discarding any potential deformation in between modalities. This strong assumption is motivated by the relaxed constraints defined for navigation accuracy. This is also motivated by the organ we target, as the pancreas is attached to the posterior abdominal wall through the posterior parietal peritoneum. In consequence, its motion is restricted due to its deep retroperitoneal position, being anchored in the C-loop of the duodenum and being delimited above by the origin of the celiac axis of the aorta. These conditions has meant that, for a very long time, it was thought that the pancreas was not subject to the movements and deformations induced by respiration for instance, in comparison with intraperitoneal organs such as the liver and the spleen, which are closer to the diaphragm (Bhasin et al. 2006). However, several studies have been carried out and prove that the pancreas deforms with respiration with movement of the pancreas in centimeter range (Gwynne et al. 2009). In these conditions, our registration accuracy results are compatible with our target and validate the developed algorithm.

Here, as we want to provide clinicians with an as simple as possible method but still medically valuable, our assumption suits the medical scenario envisioned. Before running the study described in this paper, we performed different qualitative and quantitative experiments on three other swine models (results not shown here) who helped use building insights of good accuracy performance of our system. The present

results have then been obtained on one swine model with complete set of measurements. In order to measure EUS probe pose accuracy based on our method, we have developed a specific CBCT based imaging comparison method. This allowed us to compare CT scan re-projected EUS probe to real EUS probe position. By performing such experiment, we are able to give objective re-projection error of the EUS probe and we demonstrated a shift and angle mismatch of respectively 10.4 ± 4.0 mm and $8.7° \pm 4.1°$. Even if done on limited number of targets, the ability to position the probe with an accuracy of centimeter range to match the target position, considering both calibration and registration effect combined with flexible and moving organ effect, is a clear validation of our proof-of-concept.

Nevertheless, probe registration accuracy is not enough to fully validate our approach. Here the retrieval of specific parts in the patient anatomy is of prime importance and medically relevant. Our experiment on targets retrieval in phantom have demonstrated a re-projection error of 26.2 ± 2.2 mm in phantom. This value is compatible with EUS probe pose accuracy because in this case we suffer lever effect induced by the distance of target to probe, on the order of 5 to 7 cm, as well as the inaccuracy in marble positioning in US image. Note that this result was obtained on stiff gelatin and does not represent a realistic patient. This is why we also tested our target retrieval in swine model, where we obtained an accuracy of the order of 35.9 ± 10.5 mm. This value is higher than the one reported for gelatin phantom. We noticed here a recurrent pattern where the CT scan based target position always lies in front of the retrieved EUS probe position when detected in US image. The re-projected target position in CT scan is then shifted in the direction of the US view. This apparent displacement of the fiducial based on US imaging is coherent with the EUS probe induced deformation during examination. However, this does not invalidate our methodology because we want to provide a "GPS-like" approach where EUS practitioner is given a feedback on EUS probe position and orientation, which has been demonstrated of high accuracy here, and is registered to pancreas rigid model of the patient. Once in examination, the clinician is then given an estimate of the relative position of the EUS probe to the pancreas region of interest (GPS-like feature). Then more accurate pancreas screening has to be performed based on the US image, as clinically done today.

To conclude, we obtained results compatible with our specifications for EUS probe pose first from preliminary studies in phantom and then swine models. Then the present study has been designed and ran to deliver complete accuracy estimation in position and angle. We proved our approach to give high accuracy in EUS probe pose estimation. The EUS probe to pancreas relative positioning is a useful guidance to the EUS practitioner and we believe it will help low to intermediate skilled EUS users to navigate more efficiently to the pancreas region of interest. Obtaining the real EUS probe to pancreas position is challenging due to the EUS probe pressure induced pancreas deformation and displacement. However, it does not impede EUS examination by itself. In order to validate this approach based on "GPS-like" navigation to pancreas then US based examination in a clinically relevant scenario, we will deploy an experiment focused on extensive EUS procedures analysis. This will involve multiple clinicians being asked to find some pre-implanted targets (fiducials) in swine pancreas region. Such examination, with aim to find these targets, will be performed under both with regular EUS and with our guided EUS method. Then objective comparison of participant's performance will be possible by comparing behavior and ease of use. Target matching measurement (same principle as our navigation accuracy proof study) will be performed in the same time but on a larger extent in order to give further statistical relevance to our result. This study will be conducted with a relevant

number of practitioners in order to measure performance in an objective way (time measurement, probe path length, etc.) as well as in a subjective manner with associated feedback form. This will pave the way to first-in-human clinical study in order to test our approach in daily medical practice.

Acknowledgement(s)

Special thanks to Dr MD Juan Verde (IHU) for his valuable support in phantom creation and experimental setup, to Laurent Goffin for fruitful discussions on registration and to Nicolas Delesse for valuable support with experimental setup definition.

Funding

This work was carried out within the framework of the project APEUS supported by the ARC Foundation (www.fondation-arc.org) and was partially supported by French state funds managed within the "Plan Investissements d'Avenir" and by the ANR (reference ANR-10-IAHU-02).

References

Allan M, Thompson S, Clarkson MJ, Ourselin S, Hawkes DJ, Kelly J, Stoyanov D. 2014. 2d-3d pose tracking of rigid instruments in minimally invasive surgery. In: Stoyanov D, Collins DL, Sakuma I, Abolmaesumi P, Jannin P, editors. Information Processing in Computer-Assisted Interventions; Cham. Springer International Publishing. p. 1–10.

Bhasin DK, Rana SS, Chandail VS. 2006. The pancreas and respiration: Oblivious to the obvious! Journal of Pancreas. 7(6):578–583.

Bonmati E, Hu Y, Gurusamy K, Davidson B, Pereira SP, Clarkson MJ, Barratt DC. 2017. Assessment of electromagnetic tracking accuracy for endoscopic ultrasound. In: Peters T, Yang GZ, Navab N, Mori K, Luo X, Reichl T, McLeod J, editors. Computer-Assisted and Robotic Endoscopy; Cham. Springer International Publishing. p. 36–47.

Estépar RSJ, Stylopoulos N, Ellis R, Samset E, Westin CF, Thompson C, Vosburgh K. 2007. Towards scarless surgery: An endoscopic ultrasound navigation system for transgastric access procedures. Computer Aided Surgery. 12(6):311–324.

Ferlay J, Colombet M, Soerjomataram I, Mathers C, Parkin D, Piñeros M, Znaor A, Bray F. 2019. Estimating the global cancer incidence and mortality in 2018: Globocan sources and methods. International journal of cancer. 144(8):1941–1953.

Floris I, Adam JM, Calderón PA, Sales S. 2021. Fiber optic shape sensors: A comprehensive review. Optics and Lasers in Engineering. 139:106508.

Franz AM, Haidegger T, Birkfellner W, Cleary K, Peters TM, Maier-Hein L. 2014. Electromagnetic tracking in medicine—a review of technology, validation, and applications. IEEE Transactions on Medical Imaging. 33(8):1702–1725.

Gwynne S, Wills L, Joseph G, John G, Staffurth J, Hurt C, Mukherjee S. 2009. Respiratory movement of upper abdominal organs and its effect on radiotherapy planning in pancreatic cancer1. Clinical Oncology. 21(9):713–719.

Huang J, Lok V, Ngai CH, Zhang L, Yuan J, Lao XQ, Ng K, Chong C, Zheng ZJ, Wong MCS. 2021. Worldwide burden of, risk factors for, and trends in pancreatic cancer. Gastroenterology. 160(3):744–754.

Hummel J, Figl M, Bax M, Bergmann H, Birkfellner W. 2008. 2d/3d registration of endoscopic ultrasound to CT volume data. Physics in Medicine and Biology. 53(16):4303–4316.

Jäckle S, Eixmann T, Schulz-Hildebrandt H, Hüttmann G, Pätz T. 2019. Fiber optical shape sensing of flexible instruments for endovascular navigation. International Journal of Computer Assisted Radiology and Surgery. 14(12):2137–2145.

Kikinis R, Pieper SD, Vosburgh KG. 2014. 3d slicer: A platform for subject-specific image analysis, visualization, and clinical support. New York, NY: Springer New York. p. 277–289.

Münzer B, Schoeffmann K, Böszörmenyi L. 2018. Content-based processing and analysis of endoscopic images and videos: A survey. Multimedia Tools and Applications. 77:1323–1362.

Olympus. 2022. Olympus scopeguide product webpage. [accessed 2022-07-13]. Available from: https://www.olympus-europa.com/medical/en/Products-and-Solutions/Medical-Solutions/ScopeGuide/.

van Herwaarden JA, Jansen MM, jan PA Vonken E, Bloemert-Tuin T, Bullens RW, de Borst GJ, Hazenberg CE. 2021. First in human clinical feasibility study of endovascular navigation with fiber optic realshape (fors) technology. European Journal of Vascular and Endovascular Surgery. 61(2):317–325.

Vemuri AS, Nicolau S, Sportes A, Marescaux J, Soler L, Ayache N. 2016. Interoperative biopsy site relocalization in endoluminal surgery. IEEE Transactions on Biomedical Engineering. 63(9):1862–1873.

Xiao G, Bonmati E, Thompson S, Evans J, Hipwell J, Nikitichev D, Gurusamy K, Ourselin S, Hawkes DJ, Davidson B, et al. 2018. Electromagnetic tracking in image-guided laparoscopic surgery: Comparison with optical tracking and feasibility study of a combined laparoscope and laparoscopic ultrasound system. Medical Physics. 45(11):5094–5104.